Cross-Talk Effects in the Uncertainty Estimation of Multiplexed Data Acquisition Systems

Cross-Talk Effects in the Uncertainty Estimation of Multiplexed Data Acquisition Systems

Alessio Atzori, Alessio Carullo, Simone Corbellini, Alberto Vallan

***Abstract*—This paper deals with the analysis of multi-channel data-acquisition systems with the aim of identifying and combining the main uncertainty contributions according to the GUM framework. Particular attention has been paid towards cross-talk effect, which could be an important uncertainty contribution in multiplexed data-acquisition systems. The uncertainty analysis is described for three commercial data acquisition devices highlighting that cross-talk specifications are often not suitable for a reliable uncertainty estimation in operating conditions. For this reason, an experimental set-up has been arranged to fully characterize the inter-channel effects of the investigated devices. The obtained results have highlighted that a proper characterization of a data-acquisition system is effective in estimating the actual performance at the frequency of interest and in the operating conditions for the source resistance and the input-channel configuration. Eventually, a customized procedure has been proposed that is effective in correcting the cross-talk effects also in very severe conditions of inter-channel disturbance.**

***Index Terms*—electrical quantities, data-acquisition systems, uncertainty, cross-talk**

I. Introduction

Multi-channel Data AcQuisition (DAQ) systems are largely used in research and industrial fields thanks to their flexibility and scalability. An example of application in the bio-medical field is described in [1], while [2] and [3] refer to applications for renewable energy sources. Other examples that refer to DAQ systems, which collect signals from several sensors, can be found in structural-health monitoring [4], power metering [5], environmental monitoring [6] and energy-harvester characterization [7]. Thanks to the massive production of micro-controller based boards and embedded systems, low-cost and very compact DAQ systems have been arranged that also include on-board signal-processing capabilities [8]- [9].

One of the open problems in the use of such DAQ systems consists in the correct interpretation of the uncertainty specifications provided by the manufacturers. This problem has been already highlighted in [10] and [11], where the GUM uncertainty framework [12] has been considered as a reference model for the combination of the main uncertainty contributions of a single-channel DAQ system. The same GUM approach has been compared to the numerical Monte Carlo method [13] for a low-frequency application of a single-channel DAQ system [14]. Other examples of uncertainty estimation in virtual instruments and supervisory control and data acquisition (SCADA) systems can be found in [15]- [17].

Authors are with: Politecnico di Torino - Dipartimento di Elettronica e Telecomunicazioni, corso Duca degli Abruzzi, 24 - 10129 Torino (Italy); phone: +39 0110904202, fax: +39 011 0904216, e–mail: alessio.carullo@polito.it

The uncertainty analysis of multi-channel DAQ systems requires further contributions to be taken into account, which are mainly the cross-talk among channels and the settling time for multiplexed channels [8]- [9]. Examples of estimation of cross-talk effects can be found in [18]- [19], while suitable design techniques for reducing cross-talk effects in printed circuit boards are described in [20]- [21].

Useful guide lines for the characterization of DAQ systems can be found in the standard IEEE 1057 [22], but the manufacturer specifications still remain questionable to be interpreted, above all when inter-channel effects have to be taken into account. The problem is investigated in this paper, which describes the uncertainty analysis of multi-channel DAQ systems with a particular attention towards the interaction between active channels. This manuscript is an extended version of the conference paper [23], where preliminary results that are related to this issue were described.

In the section II, the common architecture of a multiplexed DAQ system is provided and the main uncertainty contributions are identified. The GUM uncertainty framework is then implemented in the section III starting from the specifications of a commercial DAQ board. The section IV describes the experimental set-up that has been specifically conceived to characterize three different data acquisition systems, which are two commercial DAQ boards and a micro-controller based board. The obtained results are described in section V, while the final remarks are summarized in the section VI.

II. Multiplexed DAQ Systems

A. System architecture

The block scheme of a multiplexed DAQ system is shown in Fig. 1, which refers to a system that is able to acquire 16 Referenced Single Ended (RSE) signals (switch SW2 connected to ground) or 8 differential signals (MUX1 and MUX2 driven to couple channels from CH0-CH8 to CH7-CH15). Suitable circuits are usually connected to the input channels for protection of the next stages against over-current and over-voltage. One should note that the presence of the multiplexers allows the main components of the measuring chain to be shared among different channels, thus obtaining a compact and low-cost DAQ system.

The Programmable Gain Amplifier (PGA) is set to match as well as possible the amplitude of each voltage signal to the input range of the Analog to Digital Converter (ADC). The output code D of each channel is eventually processed according to the calibration function that describes the measuring chain in order to provide the measurements of the input voltage signals.

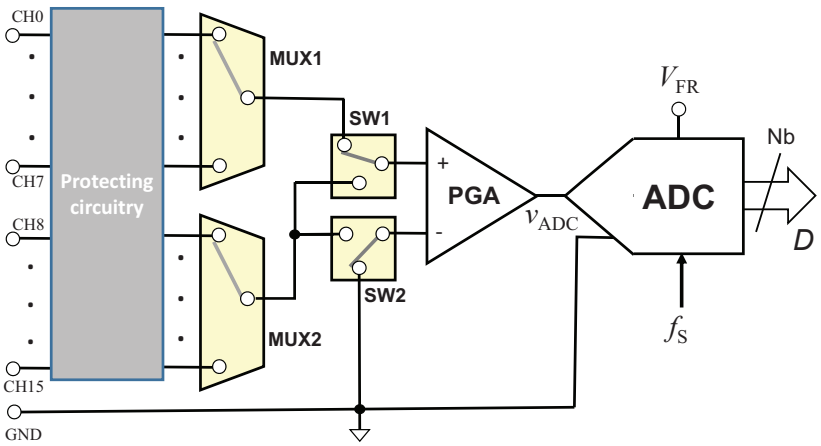

Fig. 1. Block scheme of a multiplexed DAQ system.

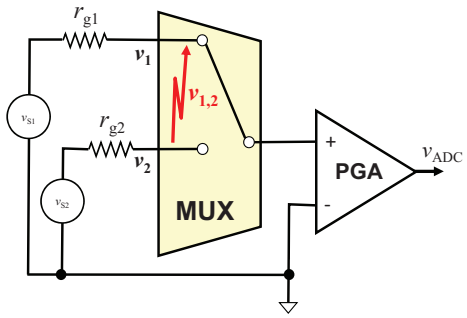

Fig. 2. The cross-talk effect in a multiplexed DAQ system.

The most important uncertainty contribution that is related to the presence of the multiplexers is the cross-talk between channels, which is defined for sinusoidal signals as:

$$CT = 20 \cdot \log_{10}\left(\frac{v_{1,2}}{v_2}\right) \quad \text{(dB)} \tag{1}$$

where $v_{1,2}$ is the root-mean square (rms) value of the disturbance that propagates to the channel 1 due to the rms-value v_2 of the signal that is present on the channel 2 (see Fig. 2 that refers to the acquisition of two signals in RSE configuration).

The estimation of the cross-talk according to the equation (1) could be a tricky problem, since it depends on the non perfect insulation between the channels of the DAQ system along the whole path (from the input connector to the MUX inputs) and between the channels of the MUXs. In addition, the cross-talk is affected by the source resistances r_{g1} and r_{g2} and by possible ground loops among the active channels, which also depend on the input configuration (RSE or DIFF).

The manufacturer specifications of commercial DAQ systems do not allow a reliable estimation of the cross-talk effect to be obtained. For low-level systems, the cross-talk is not provided and manufacturers suggest to maintain the source resistance below a certain value to have negligible cross-talk contributions. For medium-high level DAQ systems, the cross-talk is stated, but not enough details are provided to estimate the corresponding contribution in operating conditions. The source conditions are usually not specified, there is no distinction between adjacent and not adjacent channels and only a cross-talk value is provided in a specific frequency range, e.g. from DC (Direct Current) to 100 kHz, or at the upper bound of the frequency range.

The transient due to the channel switching is another important effect that is related to the presence of the MUXs. Manufacturers usually set a maximum source resistance, e.g. 1 kΩ, that allows this contribution to be made negligible. However, a suitable settling-time has to be set in order to allow the transient to be extinguished before the ADC samples the signal v_{ADC}. Such a settling-time represents a trade-off between uncertainty and sampling rate, due to the dependence of the actual sampling frequency of each channel on the settling-time value. As an example, in a four channel multiplexed DAQ system that requires a settling time of 2 μs, the sampling rate of each channel cannot be higher than 125 kSa/s, i.e. $1/(4 \cdot 2\ \mu s)$, even though the ADC can work at a higher rate. In the analysis of this paper, the assumption of settling time that minimizes the transient contribution is considered always valid.

B. Uncertainty analysis

According to the block scheme of Fig. 1, the ADC output code D_i that refers to each of the *i-th* active channels can be expressed as:

$$D_i = \frac{v_{ADC,i}}{V_q} = \frac{G_i \cdot v_i}{V_{FR}/2^{Nb}} \tag{2}$$

where G_i is the gain of the PGA for the *i-th* active channel, while V_{FR} and Nb are full-range voltage and number of bit of the ADC, respectively.

If the previous expression is rewritten highlighting the main error terms, the ADC output code that corresponds to the input channel 1 becomes:

$$D_1 = \frac{G_1 \cdot 2^{Nb} \cdot \left(v_1 + v_1^{CT} + V_{off,RTI}\right)}{V_{FR}} + D_{off} + \delta_q \tag{3}$$

where v_1^{CT} is the error term related to the cross-talk, $V_{\mathrm{off,RTI}}$ is the offset voltage Referred To Input of the PGA, D_{off} is the offset error of the ADC, and δ_{q} is the ADC quantization error.

Starting from the input/output relationship (3), the measurement of the voltage v_1 can be estimated as:

$$v_1 = \frac{V_{\mathrm{q}} \cdot D_1}{G_1} \cdot (1 + \epsilon_{\mathrm{G}}) - \left(\frac{V_{\mathrm{q}} \cdot D_{\mathrm{off}}}{G_1} + V_{\mathrm{off,RTI}} \right) + \\ - \frac{V_{\mathrm{q}} \cdot \delta_{\mathrm{q}}}{G_1} - v_1^{\mathrm{CT}} + e_{\mathrm{LE}} + e_{\mathrm{CMRR}} + n \tag{4}$$

where the term ϵ_{G} takes into account the relative error of PGA and ADC reference-voltage and the non linearity of the system, n represents the electronic noise, while the terms e_{LE} and e_{CMRR} represent the systematic effects due to the Load Effect and the Common-Mode Rejection Ratio ($CMRR$) of the PGA.

Equation (4) represents the measurement model that can be used to estimate the uncertainty of the voltage signal v_1 when the different contributions are available. However, if the DAQ system of Fig. 1 is integrated in a DAQ board or in a microcontroller chip, the characterization of the whole measuring chain is usually available and the equation (4) can be rewritten as:

$$v_1 = \frac{V_{\mathrm{q}} \cdot D_1}{G_1} \cdot (1 + \epsilon_{\mathrm{G}}) + e_{\mathrm{OFF}} + e_{\mathrm{q}} + v_1^{\mathrm{CT}} + e_{\mathrm{LE}} + e_{\mathrm{CMRR}} + n \tag{5}$$

where

$$e_{\mathrm{OFF}} = \frac{V_{\mathrm{q}} \cdot D_{\mathrm{off}}}{G_1} + V_{\mathrm{off,RTI}} \\ e_{\mathrm{q}} = \frac{V_{\mathrm{q}} \cdot \delta_{\mathrm{q}}}{G_1} \tag{6}$$

The uncertainty estimation according to the the GUM framework [12] requires that each error term of equation (5) is considered as a random variable (r.v.) and that the main systematic effects are corrected. The terms ϵ_{G} and e_{OFF} are considered r.v. with zero expected values and standard uncertainties $u(\epsilon_{\mathrm{G}})$ and $u(e_{\mathrm{OFF}})$, respectively. The term e_{q} can be also considered a r.v. with zero expected value and standard uncertainty $u(e_{\mathrm{q}}) = e_{\mathrm{q}}/\sqrt{12}$, but only if the sampling process is uncorrelated with respect to the input signal or the internal noise is larger than the quantization noise.

The systematic effect e_{LE} depends on the source impedance and on the impedance $\mathbf{Z}_{\mathrm{IN}}$ of the input channel, which is usually represented by means of a resistance R_{IN} shunted by a capacitance C_{IN}. Since R_{IN} is of the order of gigaohm and C_{IN} could be tens of picofarad, the load effect is negligible at low frequencies for source resistance up to few kiloohm, while it could be comparable to the other uncertainty contributions at high frequencies. The term e_{CMRR} is instead related to the parameter $CMRR$ of the PGA and to the Common-Mode voltage v_{CM}, which is the average of the voltages applied to the two inputs of the PGA. It could become comparable to the other uncertainty contributions if a small differential voltage is measured with a high common-mode voltage. When these two systematic effects are not negligible, their compensation has to be implemented in the calibration function and the residual uncertainty contribution has to be estimated.

The characteristics of the term v_1^{CT} depend on the possible correlation between the signal v_1 (the quantity under measurement) and the signal v_2, which is responsible for the disturbance that propagates to the adjacent channel. However, also this term can be considered a systematic effect by implementing the correction method that is proposed in the section V.D, which requires a preliminary characterization of cross-talk effects.

In the next section, a numerical example is provided that refers to a commercial DAQ board. The different uncertainty contributions are estimated and the conditions that make negligible the systematic effects e_{LE} and e_{CMRR} are defined. It will be also highlighted that the cross-talk specifications are not suitable for a reliable estimation of the corresponding uncertainty, thus requiring an experimental characterization of the DAQ Board.

III. Uncertainty estimation for a commercial DAQ board

A numerical example is here provided that refers to a commercial DAQ Board with the following specifications:

- bipolar full-range from -5 V to $+5$ V; $N_{\mathrm{b}} = 16$
- maximum sample rate: 250 kSa/s
- $\epsilon_{\mathrm{G}} = 85 \cdot 10^{-6}$; $e_{\mathrm{OFF}} = 0.2$ mV; $u(e_{\mathrm{q}} + n) = 118$ μV
- $R_{\mathrm{IN}} > 10$ GΩ; $C_{\mathrm{IN}} = 100$ pF
- $CMRR = 100$ dB (DC to 60 Hz)
- $CT = -75$ dB @ 100 kHz (adjacent channels)
- $CT = -90$ dB @ 100 kHz (non-adjacent channels)

Manufacturers usually do not provide information related to the probability distribution of gain and offset errors, then a conservative choice is made considering these r.v. characterized by uniform probability density functions (pdf) with zero expected values and upper bounds equal to ϵ_{G} and e_{OFF}, respectively. The corresponding standard uncertainties are then estimated as:

$$u(\epsilon_{\mathrm{G}}) = \frac{2 \cdot \epsilon_{\mathrm{G}}}{\sqrt{12}} \approx 49 \cdot 10^{-6}; u(e_{\mathrm{OFF}}) = \frac{2 \cdot e_{\mathrm{OFF}}}{\sqrt{12}} \approx 115 \ \mu\mathrm{V} \tag{7}$$

About the load effect of the DAQ Board on the signal source, an upper frequency limit is estimated to make the term e_{LE} negligible with respect to ϵ_{G}, i.e. $e_{\mathrm{LE}} < \epsilon_{\mathrm{G}}/4 \approx 21 \cdot 10^{-6}$. To maintain the relative load effect within this limit, for a signal source with an internal resistance not higher than 100 Ω, the signal frequency has to be lower than 100 kHz. Resistance source up to 1 kΩ can be accepted provided that the frequency is limited to 10 kHz.

The error term e_{CMRR} can be neglected (relative effect lower than $21 \cdot 10^{-6}$) if the common-mode voltage v_{CM} is not higher than the double of the differential voltage v_{D}, since $CMRR = 100$ dB. This condition is met if the input channels of the DAQ board are configured as RSE, since $v_{\mathrm{CM}} \approx v_{\mathrm{D}}/2$. In the DIFF configuration, a check has to be performed in order to verify the stated condition.

A first estimation of the relative standard uncertainty $u_{\mathrm{r}}(v_1)$, which does not include the term related to the cross-talk,

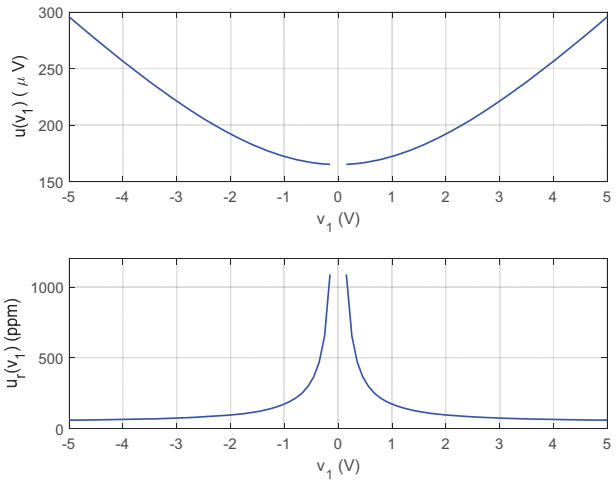

Fig. 3. Absolute (upper chart) and relative (lower chart) standard uncertainty of the measured voltage v_1 without considering the cross-talk contribution.

can be suitably obtained combining the identified uncertainty contributions. When an indirect measurement method is implemented, the matrix formalism is suggested in the GUM framework in order to easily account for possible covariance among the involved variables [24]. However, in the investigated system, where a direct measurement method is implemented, a reliable uncertainty estimation can be obtained by making suitable assumption about the correlation among the different uncertainty contributions. Since such contributions are related to quantization and noise, gain uncertainty and offset uncertainty of the measuring chain, the assumption of not significant correlation, i.e. $\rho(x_\mathrm{i}, x_\mathrm{j}) \approx 0$, seems reasonable, thus obtaining:

$$u_\mathrm{r}(v_1) = \sqrt{u^2(\epsilon_\mathrm{G}) + \frac{u^2(e_\mathrm{OFF})}{v_1^2} + \frac{u^2(e_\mathrm{q}+n)}{v_1^2}} \qquad (8)$$

In the upper chart of Fig. 3, the behavior of the absolute standard uncertainty $u(v_1)$ is shown for voltages with absolute value higher than 0.15 V. The lower chart of the same figure shows, in the same voltage range, the relative standard uncertainty $u_\mathrm{r}(v_1)$, which is included between 59 ppm and 1090 ppm. One should note as the relative uncertainty becomes very high when voltage values close to the ADC resolution are measured.

The contribution related to the cross-talk of the DAQ system has to be added to the estimated uncertainty, but the parameter CT is stated at a specific frequency (100 kHz) and the conditions for the source resistances of the involved channels are not defined. Furthermore, the cross-talk definition refers to sinusoidal signals, thus making questionable the estimation of the cross-talk contribution for arbitrary signals. For these reasons, an experimental procedure has been implemented in order to estimate the cross-talk effects in different operating conditions.

IV. Experimental set-up for cross-talk estimation

With the aim of characterizing cross-talk effects in multiplexed DAQ systems, the experimental set-up that is shown in Fig. 4 has been arranged, which refers to the RSE configuration of the input channels.

A signal generator (Tektronix AFG-3252), which is controlled via USB interface by a LabVIEW Virtual Instrument (VI) running on a PC, is connected to the input channel 2 of the DAQ system under test through a source resistance r_g2 and configured to produce sinusoidal voltage signals at different frequencies. The voltage signal on the channel 2 is set to have a peak-to-peak amplitude that is equal to the input range of the DAQ system. The input channel 1 is connected to ground through the resistance r_g1. The VI acquires voltage samples from the two active channels and process them in order to estimate the disturbance source v_2 at the input channel 2 and the error term $v_{1,2}$ at the input channel 1.

The Sampling Rate (SR kSa/s) of each channel is set to a half of the maximum sampling rate of the ADC internal to the Device Under Test (DUT) and SR samples are collected at each tested frequency, thus acquiring a frame per second for each of the two active channels. The collected samples are processed with a flat-top window and then converted in the frequency domain through a Fast Fourier Transform (FFT) algorithm using the LabVIEW module *Amplitude and Phase Spectrum.vi*. In order to obtain a reliable measurement of the rms value, repeated frames are averaged in the time domain until a minimum Signal to Noise Ratio (SNR) of 40 dB is obtained. The SNR is estimated as the ratio between the rms at the tested frequency by the rms of all the other spectral components.

The rms values of the disturbance signal v_2 and the error term $v_{1,2}$ are evaluated as the FFT modules at the index corresponding to the tested frequency. The ratio between such rms values is calculated to estimate the cross-talk according to equation (1).

To estimate the phase difference between the signals $v_{1,2}$ and v_2, the same LabVIEW module is used to find the phase values at the frequency indexes of the maximum amplitude and the estimated phase differences are unwrapped using the LabVIEW module *Unwrap Phase.vi*. The unwrapped phase difference is eventually corrected taking into account the time skew between the two active channels, which is equal to the sampling interval T_S of the ADC:

$$\Delta_\phi = \phi_1 - \phi_2 + \phi_\mathrm{corr} = \phi_1 - \phi_2 + 2\pi \cdot T_\mathrm{S} \cdot f_i \qquad (9)$$

where $T_\mathrm{S} = 1/(2 \cdot SR)$ and f_i is the tested frequency.

The same procedure is used to estimate the cross-talk effects in the DIFF configuration of the input channels of the DUT. In this case, the resistor r_g1 is connected through the first differential channel of the DUT and the disturbance signal is applied to the other differential channels.

The uncertainty of the estimated cross-talk amplitude can be obtained from the measurement model (1) propagating the uncertainty of the parameters $v_{1,2}$ and v_2. Since both parameters are the results of an FFT processing, according to

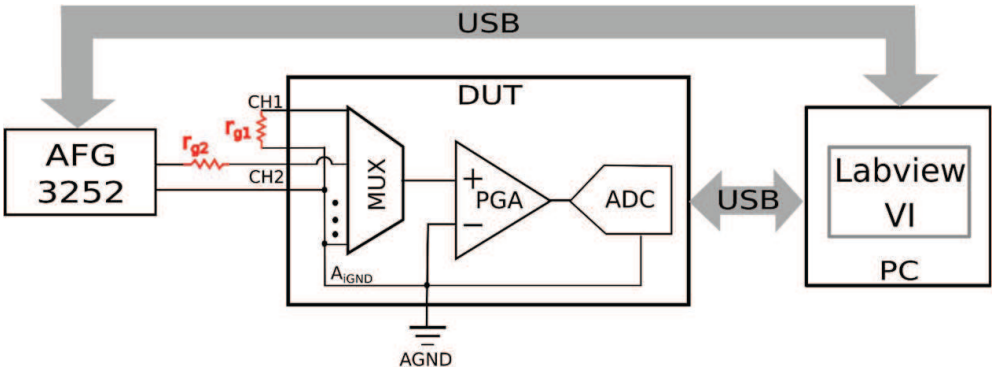

Fig. 4. Block scheme of the experimental set-up that has been arranged to estimate the cross-talk effects.

[25] the main uncertainty contribution is due to the effective number of bit B of the ADC and is expressed as:

$$u(v_{1,2}) = u(v_2) = \sqrt{3.77} \cdot \frac{u_{\mathrm{q}}}{\sqrt{2 \cdot N}} \tag{10}$$

where N is the number of processed samples, while $u_{\mathrm{q}} = V_{FR}/(2^B \cdot \sqrt{12})$. The term $\sqrt{3.77}$ takes into account the equivalent bandwidth of the flat-top window, which is used to process the acquired samples due to the non synchronous sampling here implemented.

The expression of the standard uncertainty of the cross-talk amplitude depends on the correlation that exists between $v_{1,2}$ and v_2. According to the expression (10), the corresponding uncertainty contributions depend on the effective number of bit of the ADC, which in turn mainly depends on noise and distortion. For this reason, the assumption of negligible correlation between $v_{1,2}$ and v_2 is considered, thus obtaining:

$$u(CT) = \sqrt{\left[\frac{20}{\ln(10) \cdot v_{1,2}}\right]^2 \cdot u^2(v_{1,2}) + \left[\frac{-20}{\ln(10) \cdot v_2}\right]^2 \cdot u^2(v_2)} \tag{11}$$

One should note that a different assumption for the correlation coefficient $\rho(v_{1,2}, v_2)$ in the investigated system has negligible effects, since the sensitivity coefficient of CT with respect to $v_{1,2}$ is several order of magnitude higher than the sensitivity coefficient with respect to v_2. This is related to the different order of magnitude of v_2 (about 3.5 V) with respect to $v_{1,2}$ (from about 30 μV to about 3 mV).

V. Experimental results

Thanks to the set-up described in the previous section, the cross-talk effects have been estimated for three different commercial DUTs, which are two DAQ boards and a micro-controller based board.

A. DAQ Board A

The first series of tests has been performed to characterize a commercial DAQ board hereafter referred as Board A, which is the same as the numerical example of the section III. The cross-talk estimation has been obtained in the frequency range from 100 Hz to 125 kHz. The uncertainty of the cross-talk amplitude is estimated according to the expressions (10) and (11) with an effective number of bit B that is equal to 12 and a number of samples $N = 125000$. For each tested condition, the cross-talk is reported as a couple of lines that corresponds to lower and upper bounds of the confidence interval $CT \pm 2 \cdot u(CT)$.

The results that refer to the RSE configuration of the input channels of the board are summarized in the left part of Fig. 5. The channel 1 is connected to ground through three different values of the resistance r_{g1} ($\approx$ 0 Ω, 100 Ω and 1 kΩ), while the source resistance r_{g2} is maintained at 50 Ω. The upper chart refers to the cross-talk between the adjacent channels 1 and 2, while the lower chart shows the cross-talk for non-adjacent channels 1-3 and 1-7. The manufacturer specifications for adjacent and non-adjacent channels are also shown in the two charts, which are -75 dB @ 100 kHz and -90 dB @ 100 kHz, respectively. The comparison between the manufacturer specifications and the obtained results in the tested conditions highlights that the -75 dB limit for adjacent channels is valid up to about 57 kHz for $r_{\mathrm{g1}} \approx 0$ Ω, 40 kHz for $r_{\mathrm{g1}} = 100$ Ω and 11 kHz for $r_{\mathrm{g1}} = 1$ kΩ. About non-adjacent channels, the -90 dB limit is valid up to 40 kHz for channels 1-3 ($r_{\mathrm{g1}} = 100$ Ω and $r_{\mathrm{g2}} = 50$ Ω) and up to 63 kHz for channels 1-7 ($r_{\mathrm{g1}} = 100$ Ω and $r_{\mathrm{g2}} = 50$ Ω). These outcomes highlight, as expected, a strong dependence of the actual cross-talk on the source resistances as well as an important effect of the active channels (adjacent or non-adjacent).

In the right part of Fig. 5, the results related to the DIFF configuration of the input channels of the board are summarized. Better results have been obtained in terms of cross-talk, thus showing that also the input-channel configuration has an important effect on the actual cross-talk. In this case, the -75 dB limit for adjacent channels is valid up to 95 kHz for $r_{\mathrm{g1}} \approx 0$ Ω and $r_{\mathrm{g2}} = 50$ Ω and up to 74 kHz for $r_{\mathrm{g1}} = 100$ Ω and $r_{\mathrm{g2}} = 50$ Ω. For non-adjacent channels, the -90 dB limit is valid up to 96 kHz for channels 1-3 ($r_{\mathrm{g1}} = 100$ Ω and $r_{\mathrm{g2}} = 50$ Ω) and up to 82 kHz for channels 1-7 ($r_{\mathrm{g1}} = 100$ Ω and $r_{\mathrm{g2}} = 50$ Ω).

Regardless of the cross-talk stated by the manufacturer, a frequency limit can be estimated in the tested conditions in order to consider negligible the uncertainty contribution v_1^{CT}

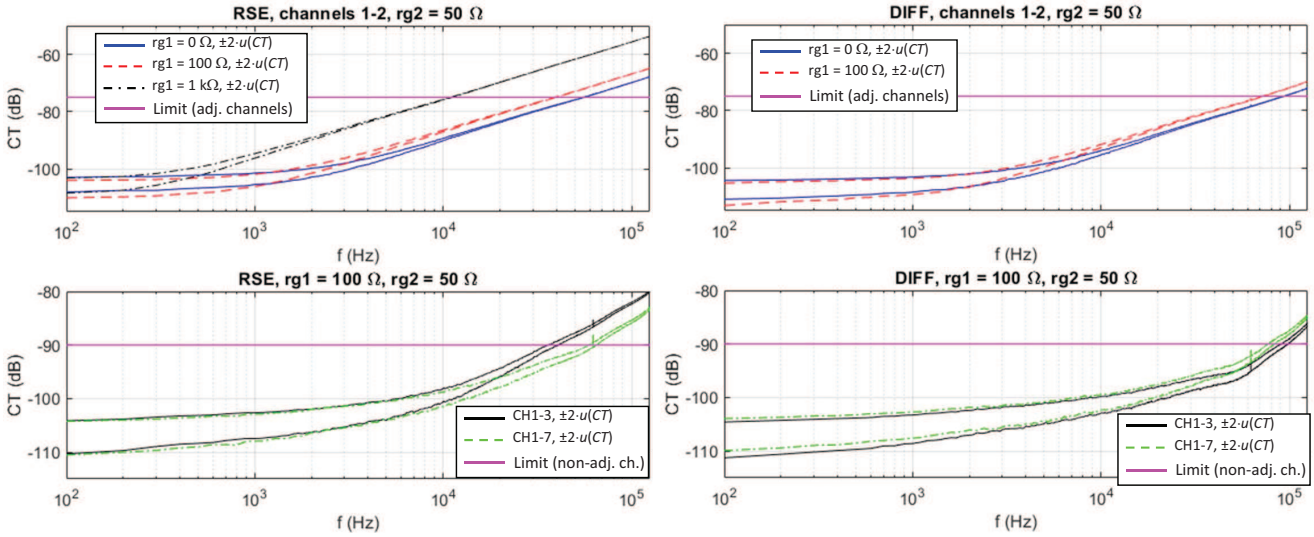

Fig. 5. The measured cross-talk for the DAQ Board A: the left part refers to the RSE configuration, while the right part refers to the DIFF configuration.

in the equation (5). Starting from the uncertainty estimation of Fig. 3, which shows a minimum standard uncertainty of about 165 μV, the standard uncertainty $u(v_1^{\mathrm{CT}})$ can be ignored if its value is not higher than 40 μV, which is about 1/4 of the minimum value of $u(v_1)$. In the worst-case scenario of a voltage signal on the channel 2 with an rms value $v_2 = 5/\sqrt{2} \approx 3.54$ V, the minimum cross-talk value is equal to:

$$CT_{\min} = 20 \cdot \log_{10}\left[\frac{u(v_1^{\mathrm{CT}})}{v_2}\right] = \\ = 20 \cdot \log_{10}\left(\frac{40 \cdot 10^{-6}}{3.54}\right) \approx -98 \text{ dB} \tag{12}$$

Taking into account this result, the cross-talk effects can be considered negligible up to the frequency values that are summarized in the Table I, which have been estimated using the upper bound of the cross-talk confidence interval.

B. DAQ Board B

The second device that has been tested is another commercial DAQ board hereafter referred as Board B, which is characterized by the specification summarized below:

- bipolar full-range from -10 V to $+10$ V; $R_{\mathrm{IN}} > 1$ GΩ; $N_{\mathrm{b}} = 16$
- maximum sample rate: 50 kSa/s
- uncertainty at full scale: 6 mV; Integral Non Linearity (INL): ±1.8 LSB
- $u(e_{\mathrm{q}} + n) = 400$ μV
- $CMRR = 56$ dB (DC to 5 kHz)

For this board, which has worse metrological characteristics than the first one, the manufacturer does not provide information related to the cross-talk effects, thus highlighting the need of a proper characterization. Only general considerations are given for multichannel applications, such as the use of short high-quality cables and impedance sources lower than 1 kΩ.

A lower bound of the expected uncertainty is estimated taking into account the contributions related to noise and quantization and to the INL. The latter is stated as ±1.8 LSB, which corresponds to a maximum voltage error of about 550 μV and then to a standard uncertainty $u(\mathrm{INL})$ (assumption of uniform distribution):

$$u(\mathrm{INL}) = \frac{2 \cdot 550 \ \mu\mathrm{V}}{\sqrt{12}} \approx 317 \ \mu\mathrm{V} \tag{13}$$

The combination of noise and INL contributions corresponds to a standard uncertainty of about 510 μV, which is considered the limit of the contribution $u(v_1^{\mathrm{CT}})$ due to the cross-talk. In the worst-case scenario (sinusoidal voltage signal on the channel 2 with an rms value $v_2 = 10/\sqrt{2} \approx 7.07$ V), the minimum cross-talk value is equal to about -82 dB (see equation (12)).

For this board, the cross-talk has been estimated in the frequency range from 100 Hz to 25 kHz, which is a half of the maximum sample rate of the internal ADC (50 kSa/s), obtaining the results that are shown in Fig. 6. The uncertainty of the cross-talk amplitude has been estimated for an effective number of bit $B = 10.7$ and a number of samples $N = 25000$. The minimum value $CT_{\min}$ that makes negligible the cross-talk effects is also shown in the figure (continuous magenta line).

About the results that refer to the RSE configuration (left part of Fig. 6), similar cross-talk values have been obtained between adjacent channels for different source resistance, since the confidence intervals are overlapped. The frequency range where the inter-channel effects do not affect the overall uncertainty has an upper bound of 9 kHz for source resistance up to 100 Ω and 8 kHz for a source resistance of 1 kΩ. Cross-talk values close to -70 dB are instead obtained at the maximum tested frequency. The cross-talk between non-adjacent channels for a source resistance $r_{\mathrm{g1}} = 100$ Ω are not distinguishable at low frequency (confidence interval between about -104 dB and -92 dB), while it increases as the frequency increases showing the lower values for the couple of channels 1-3 (about -75 dB @ 25 kHz). For this board, it should be noted that the couple of non-adjacent channels 1-4

TABLE I
FREQUENCY LIMITS THAT ENSURE A NEGLIGIBLE CROSS-TALK EFFECT FOR THE DAQ BOARD A

.

RSE ($r_{g2} = 50\ \Omega$)		DIFF ($r_{g2} = 50\ \Omega$)	
adj. channels	non-adj. channels	adj. channels	non-adj. channels
3 kHz ($r_{g1} \approx 0\ \Omega$)	14 kHz ($r_{g1} = 100\ \Omega$) CH 1-7	6 kHz ($r_{g1} \approx 0\ \Omega$)	15 kHz ($r_{g1} = 100\ \Omega$) CH 1-7
2.1 kHz ($r_{g1} = 100\ \Omega$)	11 kHz ($r_{g1} = 100\ \Omega$) CH 1-3	4 kHz ($r_{g1} = 100\ \Omega$)	16.5 kHz ($r_{g1} = 100\ \Omega$) CH 1-3

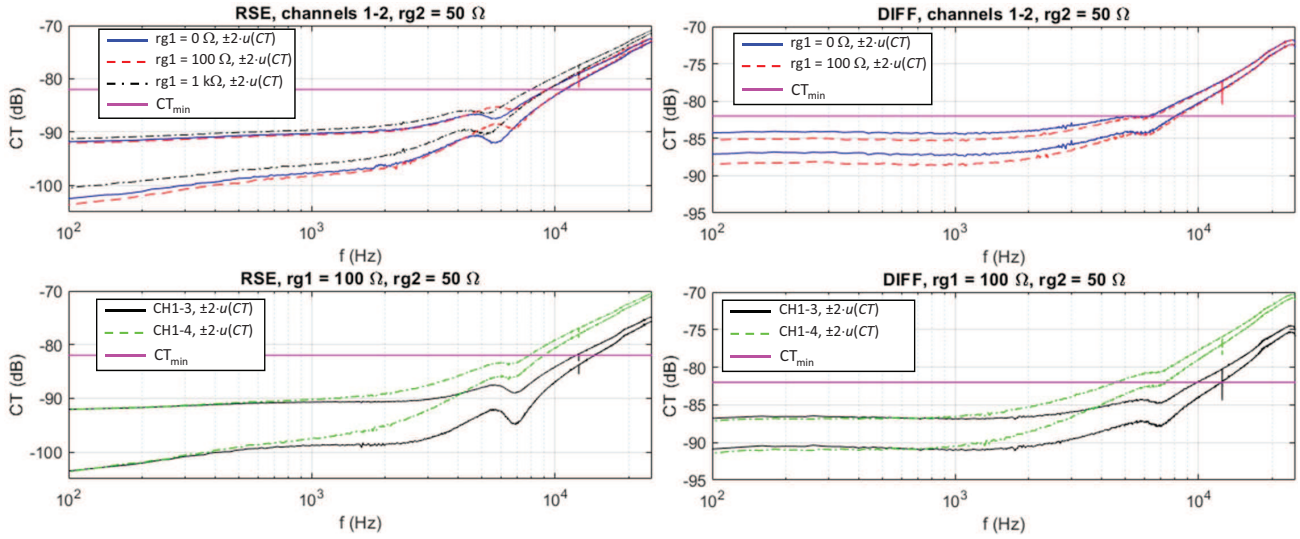

Fig. 6. The measured cross-talk for the DAQ Board B: the left part refers to the RSE configuration, while the right part refers to the DIFF configuration.

exhibits a cross-talk that is worse than the cross-talk between adjacent channels.

The results obtained for the DIFF configuration are summarized in the right part of Fig. 6, which highlights higher interference between adjacent and non-adjacent channels with respect to the RSE configuration. Cross-talk values higher than $CT_{\min}$ have been obtained for frequency higher than 6 kHz (adjacent channels, source resistance up to 100 Ω), 10 kHz (channels 1-3, source resistance 100 Ω) and 4.6 kHz (channels 1-4, source resistance 100 Ω). The non-adjacent channels 1-4 exhibit the worse behavior at frequencies higher than 4 kHz (cross-talk confidence level non overlapped with the interval of the channels 1-3), thus confirming the outcome obtained in the RSE configuration.

C. Micro-controller based board

The third device under test is a commercial development board, which embeds the micro controller Atmel SAM3X8E ARM Cortex-M3. The data-acquisition section internal to the device has an architecture that is similar to a DAQ board, including a multiplexer, a programmable gain amplifier and an ADC. The input channels can be configured both in RSE and DIFF mode. The ADC has been configured in free-running mode with a sampling rate $fs = 100$ kSa/s and with a resolution $N_b = 12$. In these conditions, the main specifications are:

- unipolar full-range V_{FR} from 0 V to 3.3 V;
- gain error: $\epsilon_G = 0.56$ %; offset error: $e_{OFF} = 11.5$ LSB; Integral Non Linearity: $INL = \pm 1.0$ LSB
- signal to Noise Ratio: $SNR = 62$ dB (single-ended mode),
  $SNR = 64$ dB (differential mode)

Also for this board, information related to the cross-talk effects is not available, but the manufacturer states the maximum source resistance that ensures a correct behavior of the Sample&Hold circuit, which depends on the sampling rate. For the selected sampling rate, the maximum source resistance is 135 kΩ for 12-bit operations.

Estimating the rms value of the noise n from the worst figure of the device ($SNR = 62$ dB) when the useful signal is a sine wave with an rms value equal to $3.3/(2\cdot\sqrt{2}) \approx 1.17$ V, the estimated noise contribution is $e_n \approx 0.92$ mV. Combining this value with the quantization noise $u(e_q) = V_q/\sqrt{12} \approx 0.23$ mV it can be obtained $u(e_q + n) \approx 0.95$ mV.

In unadjusted conditions of the ADC, the application of the expression (8) provides the results that are summarized in Fig. 7, where absolute and relative standard uncertainties of the input voltage v_{in} are shown (blue lines) in the range from 0.2 V to 3.3 V. The same figure also shows absolute and relative standard uncertainties after the compensation of the offset error of the ADC (red lines), which is one of the main uncertainty contribution.

Repeating the same considerations of the section V-A for the estimation of the minimum cross-talk value that makes the contribution v_{in}^{CT} negligible with respect to the other uncertainty contributions, values of $CT_{\min}$ equal to about -54 dB and -71 dB are obtained in unadjusted and offset-adjusted conditions, respectively.

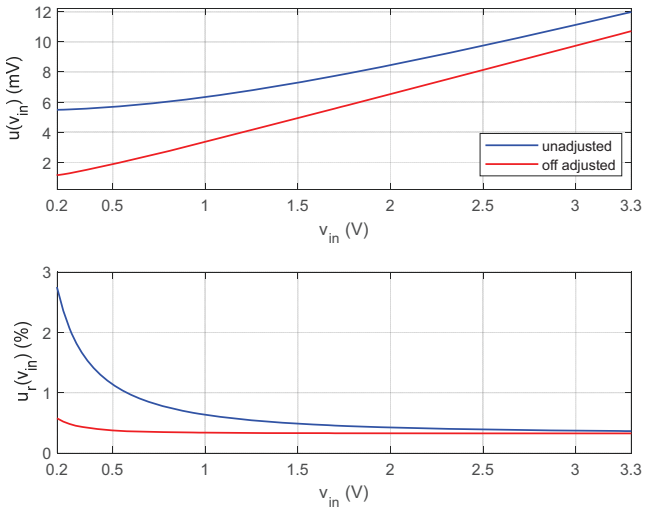

Fig. 7. Absolute (upper chart) and relative (lower chart) standard uncertainty of the input voltage $v_{\rm in}$ (range from 0.2 V to 3.3 V) for the development board in unadjusted conditions (blue lines) and after the compensation of the offset error of the ADC (red lines).

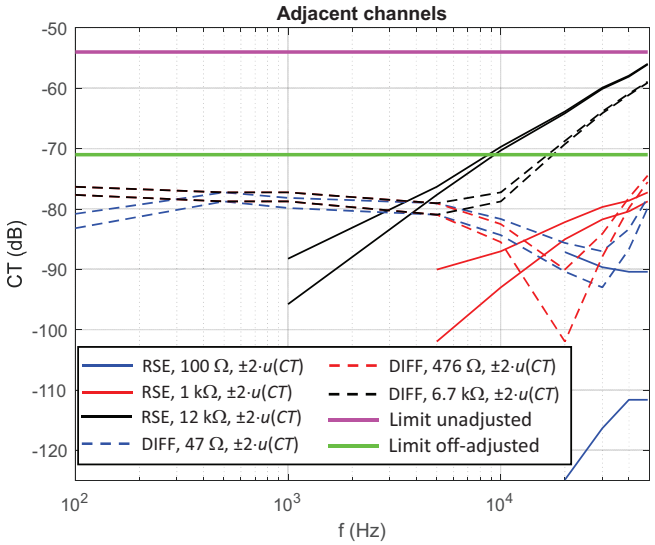

Fig. 8. The measured cross-talk among adjacent channels for the development board: continuous thin lines refer to the RSE configuration, dashed thin lines refers to DIFF configuration, while the thick lines refer to cross-talk limit in unadjusted (magenta line) and offset-adjusted (green line) conditions.

The cross-talk effects of the development board have been estimated in the frequency range from 100 Hz to 49 kHz. In RSE configuration, the gain has been set to 1 and the offset to zero for both active channels and the signal generator AFG 3252 has been set to provide a sinusoidal voltage signal with a peak-to-peak value of 3.0 V and an offset of 1.65 V. A bias voltage of about 1.65 V has been applied to the disturbed channel in RSE configuration. In DIFF configuration, both active channels have been configured with the gain set to 1 and the offset set to $V_{\rm FR}/2$, while the signal generator has been set with a peak-to-peak value of 3.0 V and an offset of 0 V. The uncertainty of the cross-talk amplitude has been estimated for an effective number of bit $B = 10$ and a number of samples $N = 49000$.

The results that refer to cross talk among adjacent input channels in RSE configuration (continuous thin lines) and DIFF configuration (dashed thin lines) are reported in Fig. 8, where also the cross-talk limits in unadjusted (thick magenta line) and offset-adjusted (thick green line) conditions are shown. One should note that in RSE configuration, reliable cross-talk measurements ($SNR \geq 40$ dB) have been obtained only at high frequencies, thus highlighting that cross-talk effects at low frequencies were similar to the noise floor. The figure shows that the cross-talk effects are always negligible in unadjusted conditions, while in offset-adjusted conditions it becomes comparable to the other uncertainty contributions for frequencies higher than 8.5 kHz (RSE, source resistance 12 kΩ) and frequencies higher than 16 kHz (DIFF, source resistance 6.7 kΩ).

The Fig. 9 summarizes the cross-talk among non-adjacent input channels (left part for channels 1-3 and right part for channels 1-4) and the line styles have the same meaning of the previous figure. Also in this case, in RSE configuration reliable cross-talk measurements have been obtained only at high frequencies and for the channels 1-4 and the source resistance 100 Ω no reliable measurements have been obtained. About the effect of the cross-talk as uncertainty contribution, it remains negligible in any configuration and in all the tested frequency range for unadjusted conditions. In offset-adjusted conditions, for the non-adjacent channels 1-3 cross-talk effects become not negligible for frequencies higher than 19 kHz (RSE, source resistance 12 kΩ) and frequencies higher than 38 kHz (DIFF, source resistance 6.7 kΩ). For the non-adjacent channels 1-4, the contribution of the cross talk has to be taken into account only in RSE configuration, for frequencies higher than 36 kHz and source resistance of 12 kΩ.

For this board, the obtained results have shown that cross-talk effects are negligible for any input-channel configuration and for source resistances up to 12 kΩ if none of the internal errors is adjusted. If instead the offset error is compensated, the uncertainty contribution due to the cross talk could become not negligible in the tested frequency range, thus suggesting a suitable configuration of the input channels and the connection to sources with low resistance.

D. Cross-talk as a systematic effect

The results obtained for the three commercial devices highlight that cross-talk effects are very different for each device and are strongly dependent on the configuration of the input channels and the source resistances. Another important outcome is the need to include the disturbance from adjacent or non-adjacent channels among the uncertainty contributions, above all at high frequencies. However, it is also possible to consider the cross-talk contribution as a systematic effect, thus correcting it during the post processing of the acquired samples.

The method here proposed, which is summarized in Fig. 10, is based on a two-step procedure: during the first step (voltage source $v_{\rm g1}$ set to zero) the characterization of the DAQ system

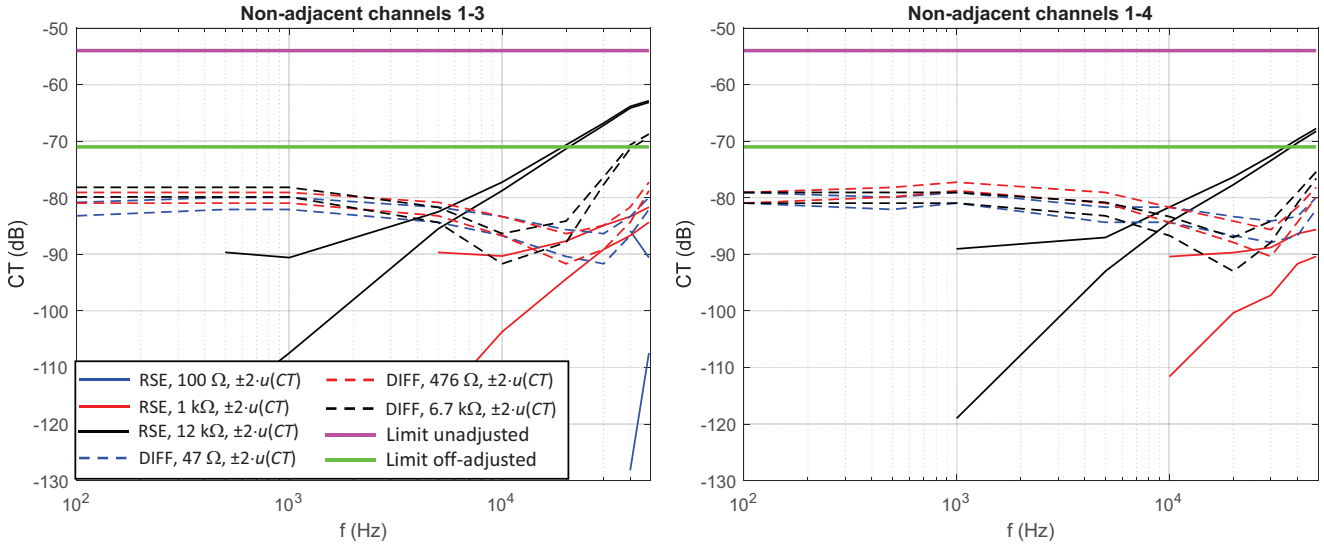

Fig. 9. The measured cross-talk among non-adjacent channels for the development board: continuous thin lines refer to the RSE configuration, dashed thin lines refers to DIFF configuration, while the thick lines refer to cross-talk limit in unadjusted (magenta line) and offset-adjusted (green line) conditions (left part for channels 1-3 and right part for channels 1-4).

in terms of cross talk is performed, while in the second step (v_{g1} turned on) the cross-talk effects are corrected.

The characterization step, which is based on the experimental set-up described in the section IV, is performed with the DAQ system in the same configuration as in the operating phase, but with no signal on the disturbed channel (CH1). In this condition, the transfer function $\hat{H}_{\mathrm{CT}}(jf)$ between the signal V_2 measured at the channel 2 and the disturbance $V_{1,2}$ is estimated at the frequencies of interest. During the normal use of the DAQ system (signal applied to CH1), the acquired samples are post-processed summing to them the inverted signal at the output of the filter $\hat{H}_{\mathrm{CT}}(jf)$. In the scheme of Fig. 10, $H_{\mathrm{CH1}}(jf)$ and $H_{\mathrm{CH2}}(jf)$ represent the transfer functions of the active channels, which in normal conditions are equal to the gain set on the two channels CH1 and CH2.

The proposed method has been implemented on the DAQ Board A in order to show its effectiveness during the measurement of a small sinusoidal signal in the presence of an isofrequential sinusoidal disturbance. The experimental set-up of Fig. 4 has been modified using two channels of the signal generator that provides two phase-locked sinusoidal signals with rms values of 100 mV on channel 1 and 7 V on channel 2. A resistor $r_{\mathrm{S}} = 100$ kΩ has been connected in series to the output channel 1 of the signal generator in order to obtain a voltage divider with the resistor r_{g1} that has an attenuation of about 1000, thus having a DAQ board input signal with an rms value of about 100 μV. In this way, a source resistance of 100 Ω is maintained, which is the same used during the characterization step. The VI LabVIEW has been also modified as shown in the Fig. 11 in order to implement the correction, for each tested frequency F(i) in the range 100 Hz ÷ 125 kHz, starting from amplitude CT(i) and phase PH(i) of the estimated cross talk. The obtained results are summarized in the left part of Fig. 12, where the continuous blue line refers to the estimated rms value at the input channel 1 when the disturbance is not present (channel 2 of the signal generator turned off), while the red dashed line is the result with the cross-talk effects not corrected. In this condition, the effect of the inter-channel disturbance is evident, with a relative rms error of about 56 % up to 10 kHz and of 1400% up to 125 kHz with respect to the non-disturbed signal. In the same chart, the dashed orange line is instead the results obtained in the presence of the disturbance on the channel 2 but with the cross-talk correction turned on. The effect of the correction is very clear in the right part of Fig. 12, with a relative rms error with respect to the non-disturbed signal that is of about 2.5 % up to 10 kHz and 16 % up to 125 kHz.

VI. Conclusions

The uncertainty of measurements provided by multi-channel DAQ systems has been estimated in this paper according to the GUM framework. Multiplexed DAQ systems have been investigated, since this architecture is commonly used to arrange compact and low-cost devices. Different uncertainty contributions have been taken into account, including the contribution that is related to the cross-talk between active channels, which becomes not negligible when a MUX is present in the measuring chain. It has been highlighted that manufacturers often do not provide enough details for a reliable estimation of this contribution in operating conditions. For this reason, an experimental set-up has been proposed that is conceived to estimate the cross-talk effect in DAQ systems in the frequency range of interest, for different resistance values of the signal source and in different configurations of the input channels (referenced single-ended vs differential, and adjacent channels vs non-adjacent channels).

Experimental results that refer to three commercial multiplexed DAQ systems have been reported in terms of measured cross-talk. Such a parameter has been compared to the other uncertainty contributions in order to identify the operating

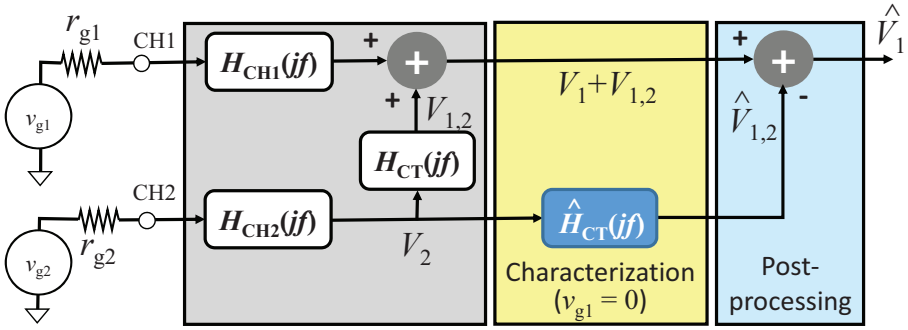

Fig. 10. Characterization (v_{g1} turned off) and correction (v_{g1} turned on) steps of cross-talk effects.

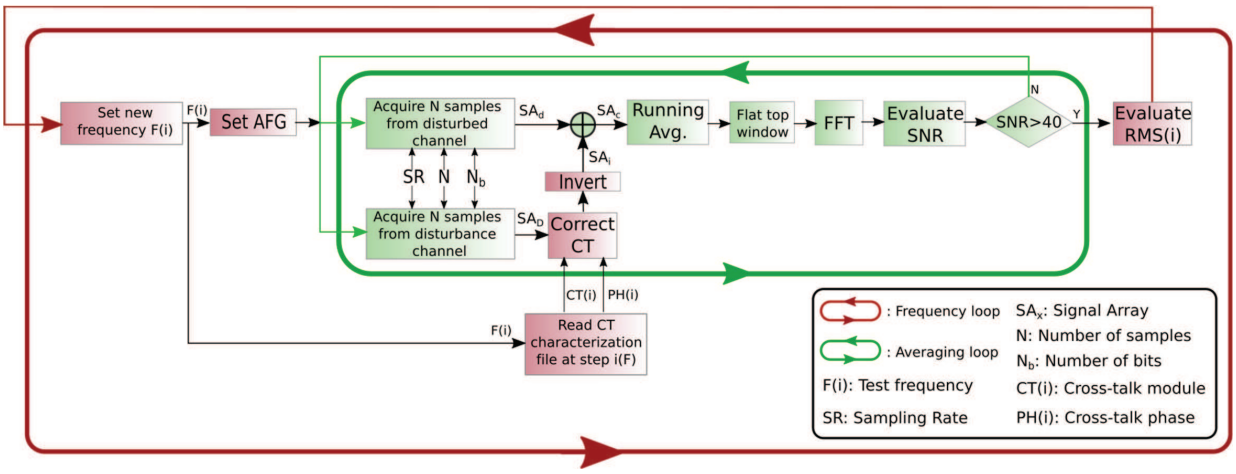

Fig. 11. Block scheme of the VI LabVIEW that implements the correction of the cross-talk effects.

conditions that make the cross-talk effects not negligible. The uncertainty of the measured cross-talk has been also evaluated, obtaining measurement intervals that are suitable for the characterization purposes. It has also been shown that the proposed procedure is effective in identifying the input configuration (RSE or DIFF) and the active channels (adjacent or non-adjacent) that minimize the cross-talk contribution.

Eventually, the authors have proposed to consider the cross-talk effect as a systematic effect, thus having the possibility to correct its contribution when it is not negligible (above all at high frequencies). With this aim, a characterization procedure has been proposed in order to identify the transfer function between a signal that is applied to an input channel and the disturbance that propagates to an adjacent or non-adjacent channel. The effectiveness of the proposed method has been shown developing a customized VI LabVIEW module that is able to implement the cross-talk correction starting from the results of the characterization of the DAQ system in operating conditions. Experimental results that refer to sinusoidal input signals in the frequency range of 100 Hz to 125 kHz have shown a reduction of the cross talk effect up to 25 dB at the highest tested frequency.

REFERENCES

[1] A. Sarkar et al., "Design and calibration of a multi-channel low voltage data acquisition system," in Proceedings of 2018 IEEE Applied Signal Processing Conference (ASPCON), December 7-9, 2018, Kolkata, India.

[2] D. Dosen, M. Znidarec and D. Sljivac, "Measurement Data Acquisition System in Laboratory for Renewable Energy Sources," in Proceedings of 18th IEEE International Conference on Smart Technologies - IEEE EUROCON 2019, July 1-4, 2019, Novi Sad, Serbia.

[3] A. Carullo and A. Vallan, "Outdoor Experimental Laboratory for Long-Term Estimation of Photovoltaic-Plant Performance,"IEEE Transactions on Instrumentation and Measurement, vol. 61(5), pp. 1307–1314, 2012.

[4] D. de Santana Nunes, J.L. Vital de Brito and G.N. Doz, "A Low-Cost Data Acquisition System for Dynamic Structural Identification," IEEE Instrumentation & Measurement Magazine, vol. 22(5), pp. 64–72, 2019.

[5] A. Cataliotti et al., "A PC-based wattmeter for accurate measurements in sinusoidal and distorded conditions: setup and experimental characterization," IEEE Transactions on Instrumentation and Measurement, vol. 61(5), pp. 1426–1434, 2012.

[6] S. Sreelal et al., "Data acquisition and processing at ocean bottom for a Tsunami warning system," Measurement, vol. 47, pp. 475–482, 2014.

[7] J.J. Ruan et al., "An automatic test bench for complete characterization of vibration-energy harvesters," IEEE Transactions on Instrumentation and Measurement, vol. 62(11), pp. 2966–2973, 2013.

[8] P.M. Pinto, J. Gouveia and P.M. Ramos, "Development, implementation and characterization of a DSP based data acquisition system with on-board processing," ACTA IMEKO, vol. 4(1), pp. 19–25, 2015.

[9] M. Abdallah, O. Elkeelany and Ali T. Alouani, "A low-cost stand-alone multichannel data acquisition, monitoring and archival system with on-chip signal preprocessing," IEEE Transactions on Instrumentation and Measurement, vol. 60(8), pp. 2813–2827, 2011.

[10] F. Alegria, P. Girao, V. Haasz and A. Serra, "Performance of data acquisition systems from the user's point of view," IEEE Transactions on Instrumentation and Measurement, vol. 53(4), pp. 907–914, 2004.

[11] D.W. Braudaway, "Uncertainty specification for data acquisition (DAQ) devices," IEEE Transactions on Instrumentation and Measurement, vol. 55(1), pp. 74–78, 2006.

[12] BIPM, IEC, IFCC, ILAC, ISO, IUPAC, IUPAP, and OIML, "Evalua-

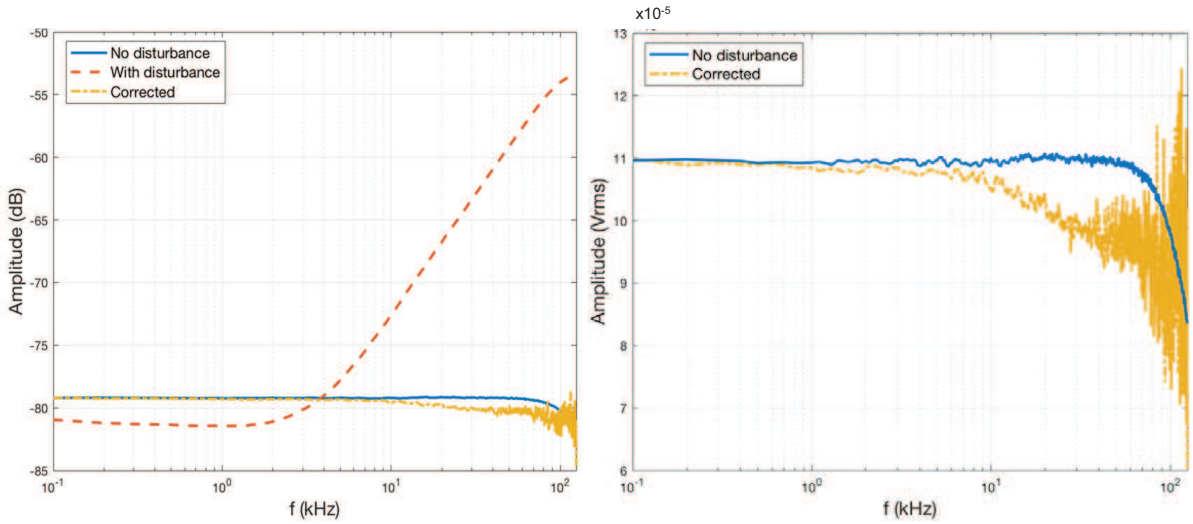

Fig. 12. The measured rms value at the input of the channel 1 of the DAQ Board A: result without disturbance (continuous blue line), result with uncorrected disturbance (dashed red line), result after the correction of the disturbance (dashed orange line).

tion of measurement data Guide to the expression of uncertainty in measurement," JCGM 100:2008.

[13] BIPM, IEC, IFCC, ILAC, ISO, IUPAC, IUPAP, and OIML, "Evaluation of measurement data - Supplement 1 to the Guide to the expression of uncertainty in measurement - Propagation of distributions using a Monte Carlo method," JCGM 101:2008.

[14] M. Catelani, L. Ciani, S. Giovannetti and A. Zanobini, "Uncertainty analysis in high-speed multifunction data acquisition device," in Proceedings of IEEE 2011 ADC Forum, June 30 - July 1, 2011, Orvieto, Italy.

[15] S. Nuccio and C. Spataro, "Approaches to evaluate the virtual instrumentation measurement uncertainties," IEEE Transactions on Instrumentation and Measurement, vol. 51(6), pp. 1347–1352, 2002.

[16] A. Baccigalupi, M. D'Arco and A. Liccardo, "Parameters and Methods for ADCs Testing Compliant With the Guide to the Expression of Uncertainty in Measurements," IEEE Transactions on Instrumentation and Measurement, vol. 66(3), pp. 424–431, 2017.

[17] S. Sinha et al., "Design and Implementation of Real-Time Flow Measurement System Using Hall Probe Sensor and PC-Based SCADA," IEEE Sensors Journal, vol. 15(10), pp. 5592–5600, 2015.

[18] S.C. Bera, N. Mandal and R. Sarkar, "Study of a Pressure Transmitter Using an Improved Inductance Bridge Network and Bourdon Tube as Transducer," IEEE Transactions on Instrumentation and Measurement, vol. 60(4), pp. 1453–1460, 2011.

[19] D. Li, G. Bianconi and S. Chakraborty, "On the Accuracy of Cross-Talk Modeling in High-Speed Digital Circuits Using the Accelerated Boundary Element Method," in Proceedings of 2020 IEEE 29$^{\text{th}}$ Conference on Electrical Performance of Electronic Packaging and Systems (EPEPS), October 5-7, 2020, San Jose, CA, USA.

[20] W. Wu, "Cross-talk interference aggressor signal frequency estimation in printed circuit boards by means of wavelet signal singularity identification," in Proceedings of 2005 IEEE International Symposium on Microwave, Antenna, Propagation and EMC Technologies for Wireless Communications, August 8-12, 2005, Beijing, China.

[21] M. Iida et al., "Reduction effects of geometrical configuration on FM-band cross-talks between two parallel signal traces on vehicle-mounted printed circuit boards," in Proceedings of 2013 Asia-Pacific Symposium on Electromagnetic Compatibility (APEMC), May 20-23, 2013, Melbourne, VIC, Australia.

[22] IEEE Standards Association, IEEE Std 1057-2017, "IEEE Standard for digitizing waveform recorders," IEEE, New York, NY (USA).

[23] A. Carullo, S. Corbellini, A. Vallan and A. Atzori, "Uncertainty Issues in Multi-Channel Data Acquisition Systems," in Proceedings of IEEE 2020 I²MTC Conference, May 25 - 28, 2020, Dubrovnik, Croatia.

[24] M. Bottaro and H. Eichinger, "Uncertainties in the heat energy calculation process and influences on determination of arc thermal performance value (ATPV) of heat- and flame-resistant materials tests," Measurement, vol. 123, pp. 275–284, 2018.

[25] G. Betta, C: Liguori and A. Pietrosanto, "Propagation of uncertainty in a discrete Fourier transform algorithm," Measurement, vol. 27, pp. 231–239, 2000.